International Journal of Engineering & Technology, 7 (4.36) (2018) 1569-1573

International Journal of Engineering & Technology

Website: www.sciencepubco.com/index.php/IJET

Research paper

Numerical modelling verification of temperature distribution in ColdArc welding of thin plate

SD Sabdin[1]*, NIS Hussein[1], MK Sued[1], Yupiter HP Manurung[2], Mohd Fadzil Jamaluddin [3]

[1] Faculty of Manufacturing Engineering, Universiti Teknikal Malaysia Melaka
[2] Faculty of Mechanical Engineering, UiTM Shah Alam
[3]Faculty of Mechanical Engineering, USM
**Corresponding author E-mail: saifulkdh@yahoo.com*

Abstract

This study investigated, Gas Metal Arc Welding of cold rolled steel plates by Cold Arc technology. The numerical modelling analysis of temperature in lap joint of two thin plates dissimilar size plates is performed with the Marcs software. The main objective from this simulation is to identify the temperature distribution in order to execute heat inputs into finite element thermal simulation of the thin plate lap joint. The analysis comprises a finite element of model for the thermal welding simulation. Moreover, the analysis includes a moving of heat source, the deposit of the materials, the temperature dependent on material properties, the condition of the boundaries as well as the melting temperature. The effects from the distribution of the heat source with the input from the energy were further examined. Additionally, the study expands the scope to the speed of the welding according to the variety of the temperatures. Therefore, predictions on reduction of welding heat input have become critically importance. Predicted by the FEM, it is demonstrated that the temperature distribution method be able to efficiently predict the welding deformation using double ellipsoidal heat source in the thin plate lap joint.

Keywords: *welding, welding joint, plate, residual stresses, stress analysis, finite element method*.

1. Introduction

Welding era is broadly utilized in automobile industries to facilitate a variety of products. It is familiar that the welding process is predicated on an intensely localized warmth enter, which has a tendency to generate undesired residual stresses and deformations in welded structures, especially regarding thin plates. Therefore, estimating the magnitude of welding deformations and distinguishing the results of the welding base on temperature distribution situations are deemed essential. Some researchers used the finite element (FE) and emerging it as a powerful approach to predict and assess the residual stress and distortions from welding [1]. However, the result from the deformations of the welding is basically associated with the temperature from the various category of manufacturing, these various categories of manufacturing consist of dimension, welding substances and welding process parameters. Therefore, unexpectedly the actual process of engineering will face several difficulties in predicting distortions from the process of welding. In many excessive temperature programs, it's miles important to enroll in collectively components of same or special chemical, physical and mechanical traits.

2. Finite element analysis

In this simulation, a three-dimensional finite element model for thermo-mechanical is coupled with the evaluation and has turned into highly developed use of MARC. Currently, the actual manufacturing system is recognized as one of the modern simulation approaches. This advance recognition is generally because of the combination of all of the aspects of thermal, mechanical and metallurgical phenomena in one analysis of lap joint distortions of shell and strong model the usage of FEM [2]. The numerical simulation makes use of the characteristics of simulated anticipation from the temperature in welding, its area, the distribution of plastic strain and welding residual stress in thin welded plates [3].

2.1. Heat Transfer

Welding is a method with sharply local heating to excessive temperature and speedy cooling afterwards. At some point of which the temperature enormously depends on the time and location, while the houses of the fabric are ranged with the prevailing temperature. Hence, the weld-induced temperature area evaluation is normally nonlinear temporary warmness transfer trouble. Throughout welding, the temperatures of the variety of elements in the weldment are immensely different
due to the nearby heating. As a result, the warmth transfer in all places during the weldment including the surrounding materials. Heat switch mechanism may be usually classed into 3 primary groups: conduction, convection and radiation. Welding temperature in skinny plate joint or shape is inevitable and regularly outcomes in lack of dimensional man- age, structural integrity and manufacturing charges increase be- cause of additional straightening paintings [4].

2.2. Material properties

Considering that the temperature gradient is quite large across the welding sector and the cloth homes change substantially, temperature structured thermal homes were applied to boom the accurate- ness of the heat transfer solution. The mechanical houses of the cold rolled have been measured experimentally, and had been additionally temperature-dependent. At the moment, the materials and its properties were not taken into consideration as the scale structured version in this examine. Thermal and mechanical residences of the material are recorded in Table 1.

Table 1: Chemical Composition of base metal

Material	C	Cr	Ni	Mn	Si	S	P
Cold Rolled	0.045	0.006	0.013	0.01	0.009	0.006	0.01

2.3. Thermal model heat source Goldak's double-ellipsoid

In this examine, the welded plates and filler fabric is regarded as a strong frame. A shifting warmth source model is evolved to pro-vide the warmth caused with the aid of the torch in the Robotic MIG welding procedure. The Goldak's double ellipsoid warmth supply version is followed to estimate volumetric warmth flux distributions as warmth enter across the welding pool [5]. The heat supply distribution is proven in Fig. 1.

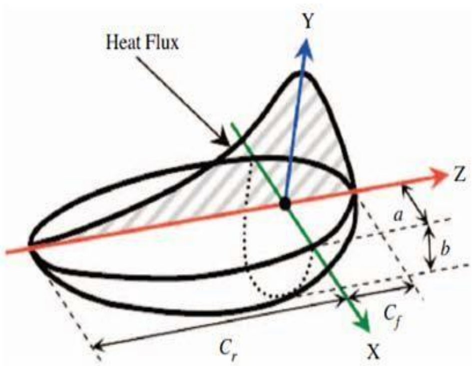

Fig. 1: Double ellipsoid heat source configurations.

This is a combination of two different ellipses where one in the quadrant is the heat source and the other in the back quadrant. The density of the two ellipsoid heat source sources, and, describes the distribution of heat flux in the front and back quadrant of heat sources can be expressed as [5]:
Distribution inside the front of the welding arc, the heat flux equation is described as:

$$q_f\,(x,y,z) = \frac{6\sqrt{3}f_f Q}{abc_f\sqrt{\pi}}\,.\,e^{-3\frac{x^2}{a^2}}\,.\,e^{-3\frac{y^2}{b^2}}\,.\,e^{-3\frac{z^2}{c_f^2}} \qquad (1)$$

Where a,b and c_f are geometric parameters as shown in figure 1, and f_f is the heat input proportion in the front part.For the (x,y and z) within the second semi-ellipsoid , covering the rear section of the arc , the rear section of the arc , the heat flux equation is described as:

$$q_r\,(x,y,z) = \frac{6\sqrt{3}f_r Q}{abc_r\sqrt{\pi}}\,.\,e^{-3\frac{x^2}{a^2}}\,.\,e^{-3\frac{y^2}{b^2}}\,.\,e^{-3\frac{z^2}{c_r^2}} \qquad (2)$$

Where a,b and c_r are geometric parameters , and f_r is the heat input proportion in the rear part and $f_f + f_r = 2$.
The distribution of fluxes in the double ellipsoid model is determined by 4 directions: Width (b), Depth (d), Rear Length (ar) and Front Length (af). The values for each direction are shown in Table 2.

Table 2: Heat source direction

Heat Source Direction	Value
Width (mm)	4
Depth (mm)	4
Forward Length (mm)	4
Rear Length (mm)	6

3. Methodology setup

The simulation was conducted according to the information obtained from literature [6] and using the welding parameters given in [7]. Selection of current, voltage and welding speed parameters are randomly based on experimental observations. The robot welding used in this study was KUKA type KRC4 with the system is equipped EWM ColdArc power source. Specimens dimension dissimilar thickness of 250 mm × 50 mm x 0.5 mm and 250 mm x 50 mmx 0.8 mm were fabricated. The material plate is JIS G 3141 Cold rolled carbon steel sheets performed on lap joint. The process of the parameters chosen for bead-on-plate experiments performed and corresponding heat input values are detailed in Table 3.

Table 3: Base material data sheet for simulation

Factors	Heat input levels		
	Low	Median	High
Welding current(A)	36	42	42
Welding voltage(V)	9	12	12
Travel speed(m/min)	0.6	0.5	0.2
Q (Kj/mm)	0.03	0.07	0.15

3.1. Simulation non-linear FEM

Potentially MSC Marc/Mentat has an ability to simulate independently from the 3rd party CAD based software since geometry can be modelled using its own platform. By searching at this simplified feature, the drawing section could be performed faster the use of MSC Marc/Mentat, although it additionally affords the import option from every other CAD software. On Fig.2 there is a simulation flow process using MSC / Marc software.

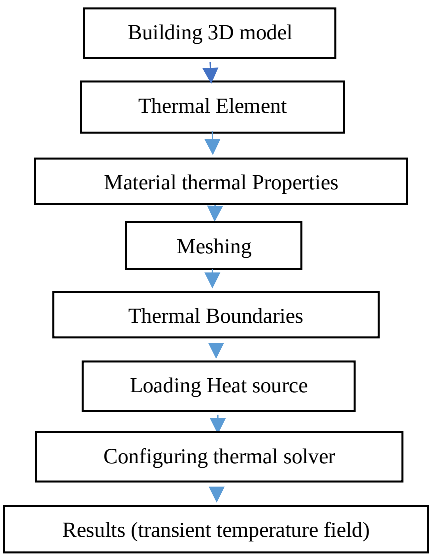

Fig. 2: Simulation framework of temperature

Fig.3 presents the developed FE model used for the thermal analysis. The green colour for grip plate clamping. The pink and orange colour for plate 1 and plate 2 . The blue ocean colour for the jig. In here shown 2 basic structure in the model is plate and table. The model has the 5 element are plate 1 on top ,plate 2 on button ,grip plate on top , support plate on button and table.

The mesh was non-linearly graded from fine to coarse size with increasing distance away from the weld centreline in fig.4. Table 4 the 8-node hexahedral brick element was applied to eliminate the negative effect of the degenerated triangle mesh during the temperature analysis. For elements with nodes that also have rotational degrees of freedom, the rotations may be additionally constrained to provide a moment carrying glue capability.

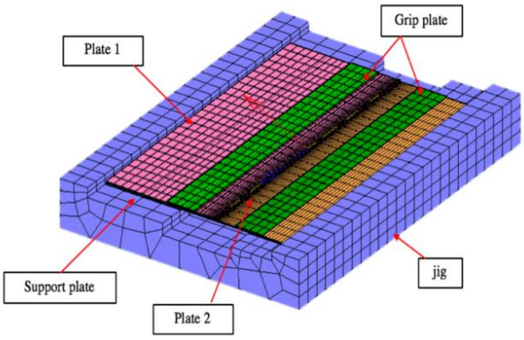

Fig.3: Finite element 3D model with table

Table 4: Element Data

Mesh	21098
Nodes	12544
Element	8554

In this simulation, the S235 steel is selected as material for the lap joint plates and filler material in table 5. The physical properties of the material are shown in Fig.5. This figure shows that the material assigned for the FEM simulation has temperature-dependent variables. These thermo-properties are most important to evaluate the model significantly base on material selection

Table 5: Base material data sheet

Material	maximum				
	C	Mn	Si	S	P
S235	0.22	1.60	0.05	0.05	0.05

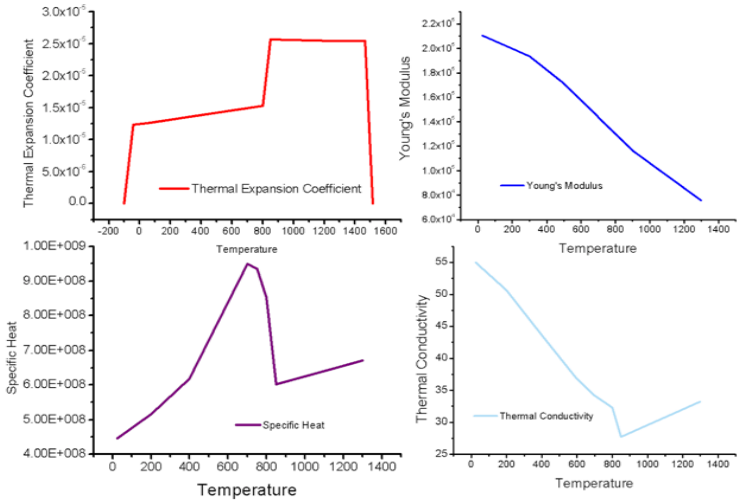

Fig. 4: Temperature-defendant thermo-physical properties of S235

As for the clamping condition, Figure 6 demonstrates the clamping placement as well as the boundary condition that is assigned within the clamping. Clamping force is applied with the direction points to negative Y direction applied for both point load clamping. The placement for both clamps are in similar locations with the experimental welding.

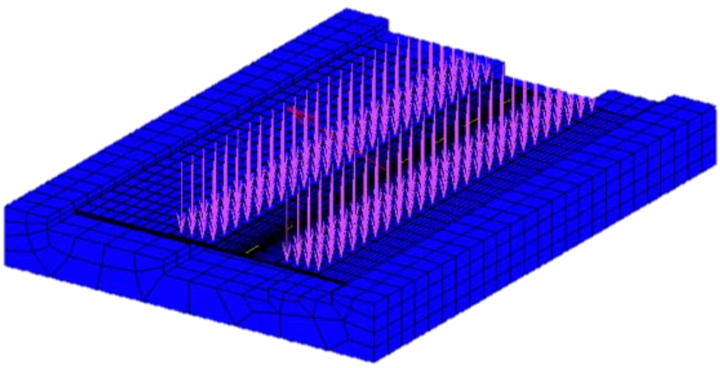

Fig.5: Clamping force on the model

4. Results and discussions

The result simulations were performed by varying the parameters of Arc voltage, Arc Current and welding speed. Fig.6 shows that each point with another point is provided with a distance of 5 mm each. Start with the middle part of the plate with a cross section to identify the temperature around the indicated zone. This allows the analyzer to analyze each zone affected by the scattered temperatures of welding process.

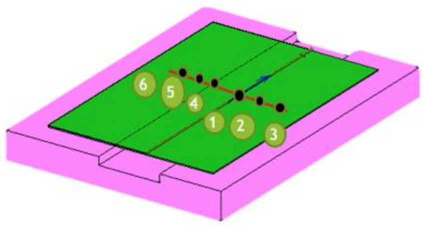

Fig.6: Schematic node point

Fig.7, 8 and 10 show the three-dimensional view of temperature distribution. This figure shows the temperature at all points marked with low , median and high heat input temperature values. Node 1 and node 4 show a high temperature increase compared to other nodes. This is because the position of this node is close to the surface of the weld toe. Fig.7 obtained the low heat input at a speed of 0.6 m / min, 9V and 36A show the increment simulation time less than 10 seconds starting the temperature rise and showing a temperature value of and show a temperature value of 979.88°C which is approaching 1000 °C at node 1.At intermediate heat input value of 0.07 kj/mm shows the increment time value at position above 10 seconds and shows the maximum temperature at 1201°C at point 1. This is at a time value of 0.5 m / min, 12 v and 42A in figure 8.Fig. 9 shows the value of heat input 0.15 kj/mm is indicating time increment exceeds 20 seconds and the maximum temperature at point 1 is 1531°C. On these three graphs show a significant value of temperature and time increment according to the values at each point. This is precisely the test that illustrates the hottest temperature value will approach the nearest weld point.

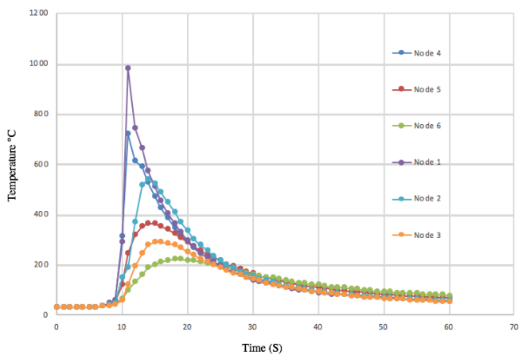

Fig.7: Temperature distribution for low heat input

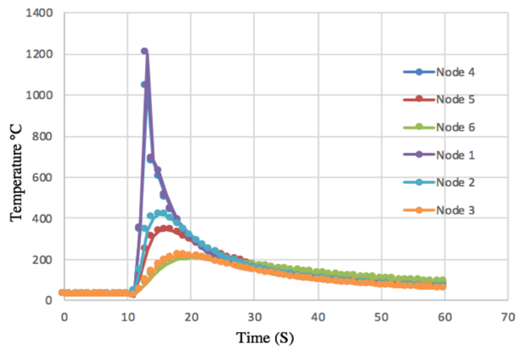

Fig.8: Temperature distribution for median heat input

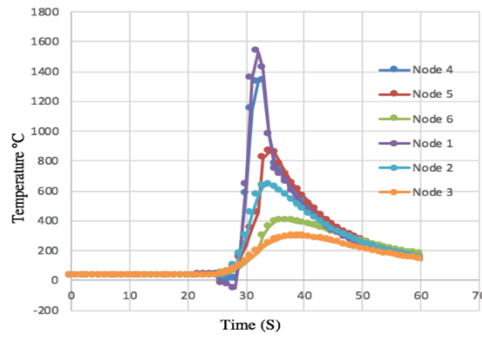

Fig.9: Temperature distribution for high heat input

It seems all the value higher heat input obtained the maximum temperature distribution for the model. The value of temperature distribution for the thin plate joint it corelate with the previous researcher [8][9].Fig. 10 shows the each node point temperature distribution. he green line represents the high heat node input velocity of 0.2 m/min. The red line represents the velocity node 0.5 m/min and the blue line has a velocity of 0.6 m/min. All lines show significant differences in their velocity spacing due to the point nodes closest to the weld toe. The position of a high parameter value indicates long distance to the front with a low and mid-value parameter. It also relates temperature to that point first in follow with another point

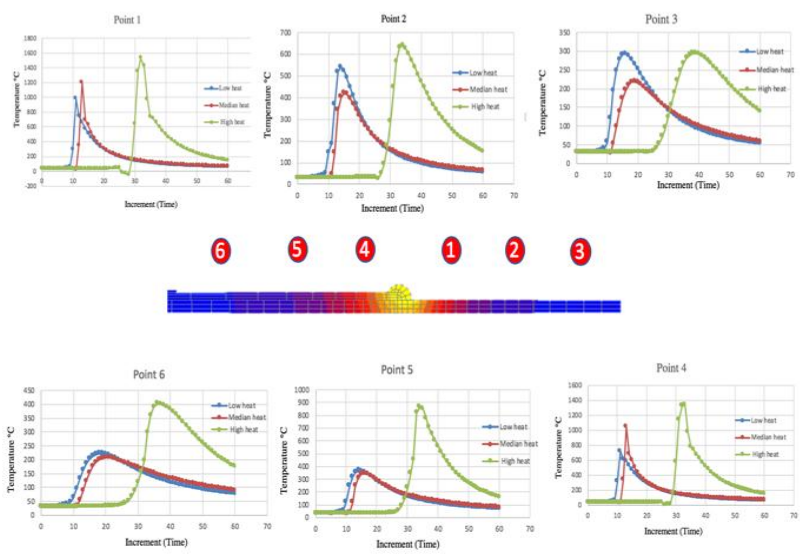

Fig.10: Temperature plot for each node

Overall the relationship between heat input and temperature distribution parallel. It seems all the value higher heat input obtained the maximum temperature distribution for the model. The value of temperature distribution for the thin plate joint it corelate with the previous researcher [8][9].
Fig. 11 show that the predicted temperature profile matches well with the weld profile and the predicted temperature history has a good agreement with the experimental one [10]. Note that This shows that the temperature in the experiment and the simulation is much the same and gives a clear knowledge of the results of this study, which is in the same temperature estimation.

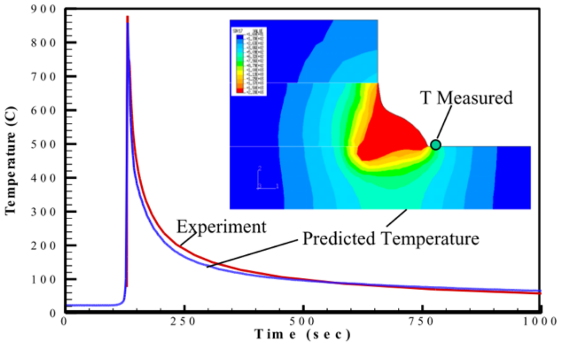

Fig.11: Comparison temperature

From the previous researcher show the maximum temperature around the welded toe reached 1,150 °C [11]. When the electrode was applied to a substrate structure, there was an immediate response consisting of a very steep temperature distribution in the vicinity of the bead generation. Subsequently, the temperature profile became smoother as the heat diffused throughout the structure. This indicates that the range of temperature found in the current position is still in the same range and therefore should emphasize research on the tight boundary conditions in carrying out real experiments in the future.

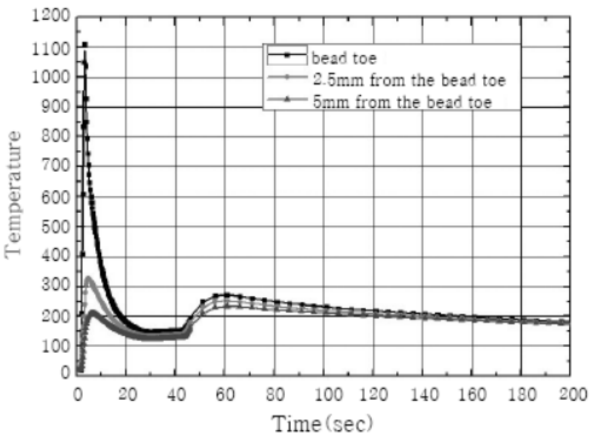

Fig.12: Temperature histories several point

5. Conclusion

Finite Element Analysis of stresses has been carried out MSC Marc/Mentat 2016. In this study 3-D FE model is developed to analyze the temperature fields and stress distribution for cold rolled thin plate. The 3-D Finite Element model which was developed have predicted temperature fields satisfactorily. After completing this work, several conclusions are made from the results shown above.

The suitability double ellipsoidal welding heat input parameter for thin plate models effected the result.
The consideration of thickness for thin plate for heat input important for temperature distribution.
The related of value heat input and temperature distribution for the model similar the result.
The simulation is very useful to analyses the variable with responses.
Low arc joining is able to help the researcher to evaluate the technology particular materials such as cold rolled.

Acknowledgement

The authors would like to thank the Faculty of Manufacturing Engineering, Universiti Teknikal Malaysia Melaka (UTeM) and AMC Faculty of Mechanical Engineering, UiTM Shah Alam for educational and technical support throughout this research.

References

[1] A. K. Dhingra and C. L. Murphy, "Numerical simulation of welding-induced distortion in thin-walled structures," *Science and Technology of Welding and Joining*, vol. 10, no. 5, pp. 528–536, 2005.
[2] M. S. Yi, C. M. Hyun, and J. K. Paik, "Three-Dimensional Thermo-Elastic-Plastic Finite Element Method Modeling for Predicting Weld-Induced Residual Stresses and Distortions in Steel Stiffened-Plate Structures," *World Journal of Engineering and Technology*, vol. 06, no. 01, pp. 176–200, 2018.
[3] D. Deng and H. Murakawa, "Prediction of welding distortion and residual stress in a thin plate butt-welded joint," *Computational Materials Science*, vol. 43, no. 2, pp. 353–365, 2008.
[4] D. Deng, Y. Zhou, T. Bi, and X. Liu, "Experimental and numerical investigations of welding distortion induced by CO2 gas arc welding in thin-plate bead-on joints," *Materials and Design*, vol. 52, pp. 720–729, 2013.
[5] J. Goldak, A. Chakravarti, and M. Bibby, "A new finite element model for welding heat sources," *Metallurgical Transactions B*, vol. 15, no. 2, pp. 299–305, 1984.
[6] M. De Dompablo, "New solutions in coldArc and forceArc welding technology," *Welding International*, vol. 27, no. December 2014, pp. 37–41, 2013.
[7] P. Miguel, S. Almeida, and N. Titanium, "Innovations in arc welding," *5º Congresso Luso-Moçambicano de Engenharia*, no. April 2016, 2011.
[8] M. Hashemzadeh, B.-Q. Chen, and C. Guedes Soares, "Comparison between different heat sources types in thin-plate welding simulation," *Developments in Maritime Transportation and Exploitation of Sea Resources - Proceedings of IMAM 2013, 15th International Congress of the International Maritime Association of the Mediterranean*, vol. 1, no. 2004, pp. 329–335, 2014.
[9] S. Stano, T. Pfeifer, and M. Różański, "Modern technologies of welding aluminium and its alloys," *Welding International*, vol. 28, no. 2, pp. 91–99, 2014.
[10] C. Paper, "Weld Modeling Procedures Development of Lap Joint," no. August, 2000.
[11] S.-Y. Hwang, J.-H. Lee, S.-C. Kim, and K. K. Viswanathan, "Numerical Simulation of Welding Residual Stress Distribution on T-joint Fillet Structure," *International Journal of Ocean System Engineering*, vol. 2, no. 2, pp. 82–91, 2012.